Journal of Integrative Agriculture 2016, 15(5): 1145–1156

Available online at www.sciencedirect.com

ScienceDirect

RESEARCH ARTICLE

Vegetation changes in the agricultural-pastoral areas of northern China from 2001 to 2013

SU Wei[1, 4], YU De-yong[1], SUN Zhong-ping[2, 3], ZHAN Jun-ge[4], LIU Xiao-xuan[4], LUO Qian[4]

[1] *State Key Laboratory of Earth Surface Processes and Resource Ecology, Beijing Normal University, Beijing 100875, P.R.China*
[2] *State Key Laboratory of Remote Sensing Science/School of Geography, Beijing Normal University, Beijing 100875, P.R.China*
[3] *Satellite Environment Center, Ministry of Environmental Protection, Beijing 100094, P.R.China*
[4] *College of Information and Electrical Engineering, China Agricultural University, Beijing 100083, P.R.China*

Abstract

Climate change and human activity have resulted in increasing change of vegetation growth globally. Numerous studies have been conducted on extreme climate events and analyses of ecological environment evolution. However, such studies have placed little emphasis on vegetation change and spatial variation in this type of ecotone. Accordingly, this study analyzed the changes in vegetation type and growth using the 16-d composite MOD13A1 product with 1-km resolution and MOD12Q1 product with 1-km resolution. We used the mean, maximum, standard deviation normalized-difference vegetation index (NDVI) values, and the rate of change (ROC) of NDVI value to explain vegetation changes within the studied ecotone. Our results showed that significant vegetation type and growth changes have occurred in the study area. From 2001 to 2013, for example, with the exception of 2001, 2004 and 2009, a certain extent of grassland area was converted to cropland. Drought severity index (DSI) results indicate that there exists drought in 2001, 2004 and 2009. Such temporal changes in cropland and grassland area confirmed the ecological vulnerability of the ecotone. At the same time, vegetation varied spatially from west to east and from south to north. The mean, maximum and standard deviation NDVI values were all sorted in descending order based on differences in latitude and longitude, as follows: $NDVI_{2013}$>$NDVI_{2009}$>$NDVI_{2004}$>$NDVI_{2001}$

Keywords: vegetation growth, agricultural-pastoral area, MODIS, land cover change, temporal change, spatial variation

1. Introduction

In recent years, global climate change and human activity have affected physical and biological systems (Battisti and Naylor 2009; Karnieli *et al*. 2014), particularly in semiarid regions where exist rising temperatures, more frequent drought events and changes in precipitation regimes (John *et al*. 2009) since the 1970s (Ford and Pearce 2010). Vegetation change is one of the dominant dynamic responses of terrestrial ecosystems to climatic changes (Richardson *et al*. 2013). Therefore, numerous researchers studied the response of vegetation to climate change, they found clear evidence of ecological and climate gradients in ecotone zones (Kent *et al*. 1997; Rudel *et al*. 2005). Their findings indicated that ecological environments within ecotone zones are fragile (Attrill and Rundle 2002).

Received 21 April, 2015 Accepted 24 August, 2015
SU Wei, E-mail: suwei7963@163.com; Correspondence SUN Zhong-ping, Tel: +86-10-58311572, Fax: +86-10-58311501, E-mail: sunnybnu114@163.com

doi: 10.1016/S2095-3119(15)61159-5

Agricultural-pastoral ecotones are defined as transitional zones between agricultural and pastoral areas (Dong *et al*. 2011) where cropland and grassland husbandry overlap both spatially and temporally. Many agricultural-pastoral areas exist in China, such as those in northern China, the semiarid ecotones of southwestern China and the oasis-desert transitional zones in arid regions of northwestern China (Zhao *et al*. 2002). Among these, agricultural-pastoral areas in northern China are the most fragile transitional zones in China. This area is a semiarid region owing to their low annual precipitation (250–500 mm). In addition, this type of region is very sensitive to the change of rainfall and temperature. In recent years, land degradation in this zone has been the largest and the longest in spatial scale compared to other ecotone areas in China. Therefore, many researchers have studied climate and land use changes in this ecotone from the 1970s onwards because of the serious desertification and deterioration of its ecological environment that have occurred (Dong *et al*. 2010).

Some researches on climate change and land cover type change have taken place in the agricultural-pastoral area of China. Gong and Han (2004) studied extreme climate events and related trends from 1956 to 2001. They found that the number of days of heavy rain, drought, and high temperatures increased during this period. Similarly, Zhang and Liu (2003) analyzed the spatial distribution of precipitation extremes in these areas and derived the same conclusions. Dong *et al*. (2007) monitored the changes in cultivated land in this ecotone using Landsat thematic mapper (TM) and multispectral scanner (MSS) remote-sensing images from 1975, 1985, 1995, 2000, and 2005. They found that the decreasing of cultivated land was primarily the result of the abandonment of cultivated land (before 2000), establishment of forest and increase in grassland (after 2000) as well as factors such as desertification and salinization. Chen *et al*. (2008) and Liu *et al*. (2011) studied land use/cover changes and found that there is a rise in temperature, a decrease in precipitation and a change of land cover type in most parts of this area.

Vegetation and its surrounding climate influence each other on timescales ranging from seconds to millions of years (Sellers *et al*. 1995; Tao *et al*. 2010, 2014). Unfortunately, only limited data is available on the response of dominant vegetation types on climate change and human activity in this ecological area, especially in the last several decades. As a consequence, we do not currently understand how changes in land cover type and agricultural and grassland boundaries correspond to climate change, how vegetation growth will be affected, and whether all vegetation types change in a similar manner, which are all important indicators of changes in the ecological environment. Furthermore, it is important for us to understand the similarities and differences in these changes along latitudinal and longitudinal gradients in this ecologically fragile region. Accordingly, the present study concentrated on monitoring and analyzing changes in vegetation growth in this region.

Specifically, we analyzed the changes in two dominant land types (cropland and grassland), and by determining changes in their boundaries since 2001, examined the relationships between vegetation growth and climate factor change. Our objectives were to report the vegetation change since 2001, and clarify the relationship of the vegetation to climate factor change in this fragile ecotone.

2. Results and discussion

2.1. Precipitation and temperature change

The amount of precipitation and temperature affect the vegetation growth seriously. So we analyzed the precipitation and temperature change before vegetation change analysis. Fig. 1-A is the moving track of precipitation centroid from 2001 to 2013, which shows that the precipitation centroid in 2001, 2004, 2009, and 2013 move to the south area with 41.07, 41.25, 40.89, and 41.17°N in latitude, respectively. This indicates that there is less precipitation in these years. And Fig. 1-B is the temperature change result in study area from 2001 to 2013, we can find that the temperature is dropped in this period.

2.2. Change in the area of vegetation

There are eight land cover types identified within the study area: forest, shrub land, grassland, wetland, cropland, urban areas, snow and ice areas, and bare land. The dominant land cover type was grassland, followed in descending order by cropland and forest. Significant changes in land cover types were found in the study area between 2001 and 2012, and there was an obvious change from grassland to cropland. Cropland was distributed in the southern (primarily in a number of counties in the central region of Gansu Province), the central (primarily in a number of counties in Liaoning Province and in the Inner Mongolia Autonomous Region) and the northern regions (Heilongjiang Province) (Fig. 2). Fig. 2 shows that the cropland area was converted to grassland in these three areas, and that the boundary of the cropland area moved into what was originally grassland. These new cropland areas created by this land cover change process were adjacent to original cropland areas and were not distributed independently.

Table 1 shows that the grassland area decreased from 562 911 to 510 240 km^2 between 2001 and 2012, and the proportion of the area decreased from 75.4 to 68.3%. Conversely, cropland mosaic area increased from 103 002 to 157 623 km^2 during this period, and its proportion of the

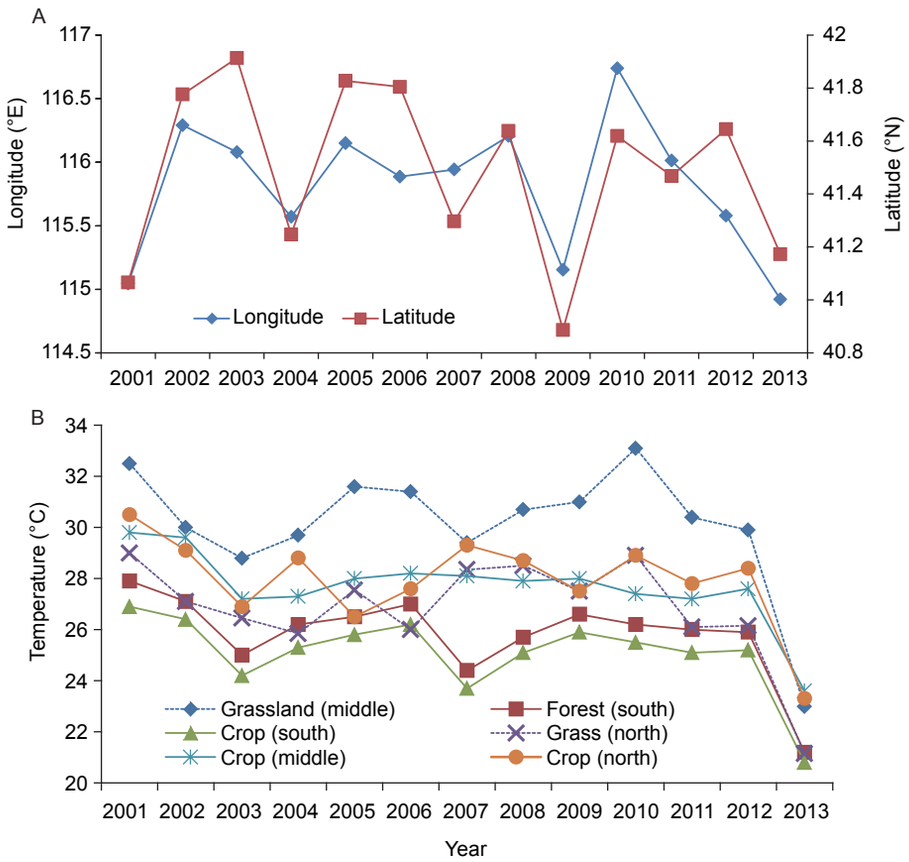

Fig. 1 Precipitation and temperature change in study area.

area increased from 13.8 to 21.1%. The cropland/natural vegetation increased from 12717 to 15483 km^2 (i.e., from 1.7 to 2.1% of the area). In addition, under the Chinese national policy of consolidating the work of converting farmland back into forest which is proposed in 2008–2011, the forest area was greater in 2012 than in 2001, with an increase from 26026 to 40285 km^2. However, the proportion of the area as forest remained low, with an increase from 3.5% in 2001 to only 5.4% in 2012. Table 1 shows a greater increase in cropland area and a decrease in grassland area between 2001 and 2012. In addition, we found that the area of mixed forest increased and that of shrub land decreased during this period, which can be clearly seen in Table 1.

Fig. 3 compares the areas of cropland and grassland during the study period. It shows that the grassland area decreased from 2001 to 2004, increased from 2005 to 2009, and decreased again from 2009 to 2012. Conversely, the cropland area increased from 2001 to 2004, decreased from 2005 to 2009, and increased again from 2009 to 2012.

As an indicator of terrestrial water availability and associated wetness or drought, drought severity index (DSI) product is computed on a gridcell-wise evapotranspiration (ET) and potential evapotranspiration (PET). The DSI is a dimensionless index ranging theoretically from unlimited negative values (drier than normal) to unlimited positive values (wetter than normal) (Mu *et al*. 2013). So we used DSI images to explain why the grassland and cropland area fluctuated within 2001, 2004, 2005, and 2009, which is showed in Fig. 4. We can see that there is more serious drought in 2001 than 2004 for grassland area, which results in decreased grassland. At the same time, there is more serious drought in 2004 and 2005, so the cropland area decreases.

2.3. Temporal changes in the main vegetation types

We analyzed vegetation cover changes in areas with and without land type change from 2001 to 2013. First, we selected six different sample areas without land type changes with the aim of monitoring changes resulting from climate factor change only: cropland areas located in the southern, central and northern sections of the study area, grassland areas located in the northern and central sections, and forest located in the southern section. The six sample areas covered three of the main vegetation types within different longitudinal and latitudinal zones in the ecotone.

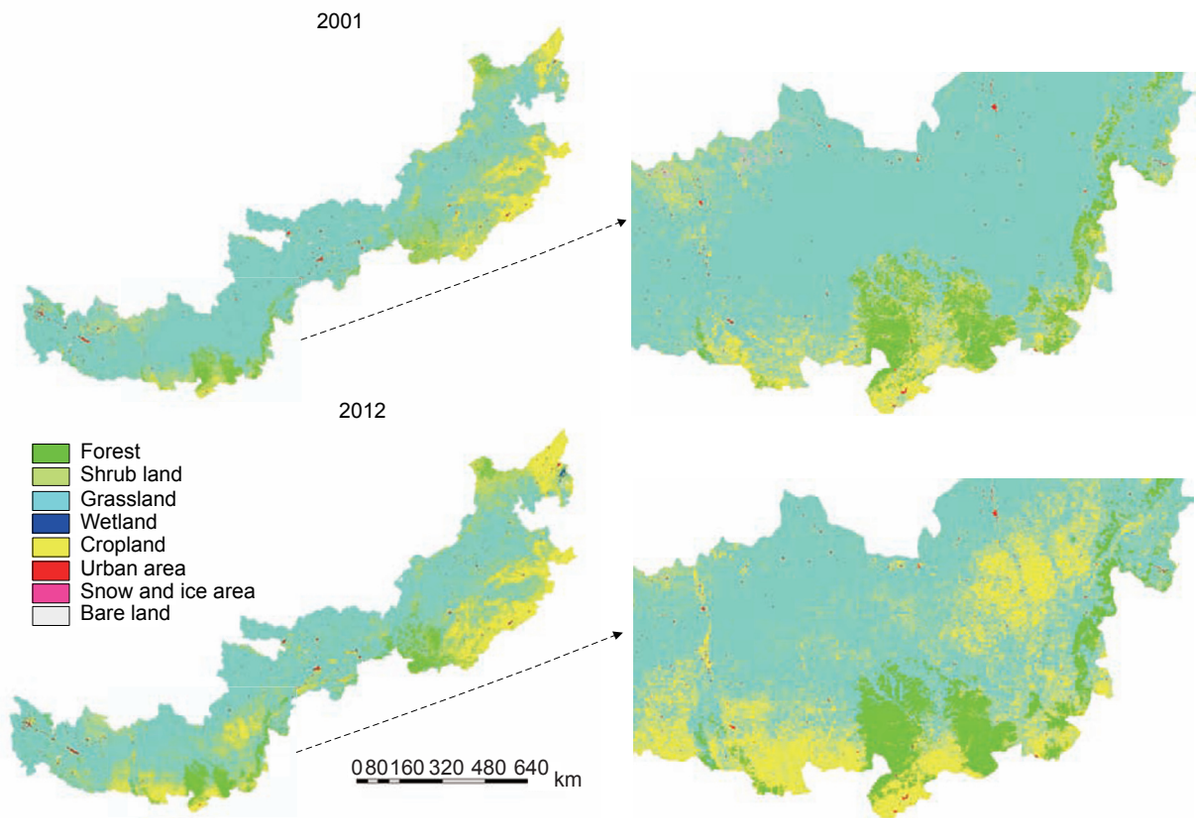

Fig. 2 The 2001 and 2012 land cover type maps.

Fig. 5 shows the changes in the 16-d normalized-difference vegetation index (NDVI) time series from 2001 to 2013 in the six sample areas. It shows obvious inter-annual fluctuation for the main vegetation types, but with different ranges of fluctuation. Cropland experienced very large changes. Moreover, cropland in the northern section of the study area had the highest fluctuations. This was due to its greater vulnerability to changes compared to crops in the central and southern sections. In comparison, changes in the southern and central cropland areas were smaller (i.e., NDVI was more stable). Almost all NDVI values were higher than 0.2 for cropland areas located in the southern part, and only during certain periods NDVI values for cropland in the central section were less than 0.2. Grassland areas in the northern and central sections of the ecotone had the lowest NDVI values between 2001 and 2013, and exhibited significant changes in these values.

We also selected some sample areas with land cover type changes to analyze the changes resulting from climate factor change and human activity using the rate of change (ROC) values. Fig. 6 shows the ROC value of NDVI for different patterns of vegetation change from 2001 to 2013, there are 23 ROC values for every year which resulting from 16-d compositing NDVI product. Fig. 6-A illustrates the changes in NDVI for forest that remained forest, and showed natural annual fluctuations. In contrast, Fig. 6-B shows the changes where the vegetation changed from grassland to cropland. Large changes in vegetation growth occurred in these areas, especially in 2009, when the lowest ROC value was −0.25 and the highest was 0.4. Fig. 6-C clearly shows more frequent (occurring almost once per year) and greater vegetation growth changes (from −0.3 to 0.4) than in the other land cover types. These results confirm that grassland, cropland and mixed-use areas experience greater fluctuation than other land cover types.

2.4. Spatial variation of vegetation

To explain the spatial variation of vegetation, we analyzed latitudinal and longitudinal changes in NDVI in 2001, 2004, 2009, and 2013, during periods whose precipitation centroid shift to south compared with other years. Fig. 7-A shows the profile for NDVI changes from west to east and south to north in the ecotone. It includes cropland and grassland with and without changes in land cover, forest, shrub land, and urban areas.

The greatest changes occurred from 36 to 38.5°N, with the land cover type changing from grassland in 2001 to cropland in 2013. Between these latitudes, the mean NDVI varied from 0.16 to 0.34 (Fig. 8-A), the maximum NDVI var-

Table 1 The areas and proportions of the total area for the main land cover types in the study area

Type	2001	2002	2003	2004	2005	2006	2007	2008	2009	2010	2011	2012
Mixed forest												
Area (km^2)	26026	21751	24036	24627	26316	24093	22454	27090	29657	31882	30497	40285
Proportion (%)	3.49	2.91	3.22	3.30	3.52	3.23	3.01	3.63	3.97	4.27	4.08	5.40
Shrub land												
Area (km^2)	16612	14404	16234	21668	22571	24550	24380	31402	23127	21180	11338	9621
Proportion (%)	2.22	1.93	2.17	2.90	3.02	3.29	3.26	4.21	3.10	2.84	1.52	1.29
Grassland												
Area (km^2)	562911	539412	560652	520348	545165	547094	554503	553793	565109	551534	549922	510240
Proportion (%)	75.38	72.23	75.08	69.67	73.01	73.26	74.26	74.16	75.67	73.85	73.64	68.33
Cropland												
Area (km^2)	103002	143044	122983	156464	127276	120790	114991	106991	104534	118884	127523	157623
Proportion (%)	13.79	19.15	16.47	20.95	17.04	16.17	15.40	14.33	14.00	15.92	17.08	21.11
Cropland/natural vegetation mosaic												
Area (km^2)	12717	11385	9653	11557	8037	8227	8044	9561	9851	8729	9088	15483
Proportion (%)	1.70	1.52	1.29	1.55	1.08	1.10	1.08	1.28	1.32	1.17	1.22	2.07

ied from 0.22 to 0.65 (Fig. 8-C), and the standard deviation of NDVI varied from 0.07 to 0.17 (Fig. 8-E). In addition, the mean, maximum and standard deviation NDVI values were all sorted as follows: $NDVI_{2013}$>$NDVI_{2009}$>$NDVI_{2004}$>$NDVI_{2001}$. These patterns could be the result of the effects of climate factor change on vegetation and land cover. As shown in Fig. 8-A, C, and E, all three NDVI parameters increased between 2001 and 2013 moving from west to east. This could be the result of climate and land cover changes as well as the increase in vegetation growth during the study period. We also observed clear changes along the longitudinal transect (Fig. 8-B, D and F), although the patterns differed from those along a latitudinal gradient. We also observed changes along the longitudinal gradient, but the changes were not distinct within this period.

3. Conclusion

In this study, we analyzed vegetation growth changes in the agricultural-pastoral areas of northern China using moderate resolution imaging spectroradiometer (MODIS) NDVI values obtained from 2001 to 2013. We reached the following main conclusions.

Land cover type changes were identified From 2001 and 2012, a certain amount of grassland was converted to cropland. Increasing forest cover in the ecotone resulted from China's policy of returning farmland to forest. Influenced by the decreasing precipitation in 2001, 2004 and 2009, a certain amount of cropland degenerated into grassland.

Vegetation growth change is affected by climate factor change and human activity For areas without changes in the land cover type, clear interannual fluctuation in NDVI occurred, but with different fluctuation ranges. Forest had the highest NDVI values and experienced little annual change, confirming its resistance to climate change. Cropland was most sensitive to climate factor change, and exhibited large annual changes in NDVI, especially in 2009, when a serious drought occurred in the ecotone. For areas that experienced land cover type change, including the conversion of grassland to cropland and changes in the cover types in areas with a mixture of land uses, greater vegetation growth changes occurred. Therefore, we conclude that areas with fragmented land cover types were more vulnerable to climate factor change.

Clear latitudinal and longitudinal variations in NDVI patterns in this ecologically fragile region were shown Along the latitudinal gradient, greater changes occurred in areas where land cover type changed, particularly for the conversion from grassland to cropland, than in areas without a change in land cover type. In addition, the standard deviation of NDVI increased over time, possibly as a result of greater fragmentation of land cover types between 2001 and 2013.

4. Materials and methods

4.1. Study area

The agricultural-pastoral areas of northern China are mostly located

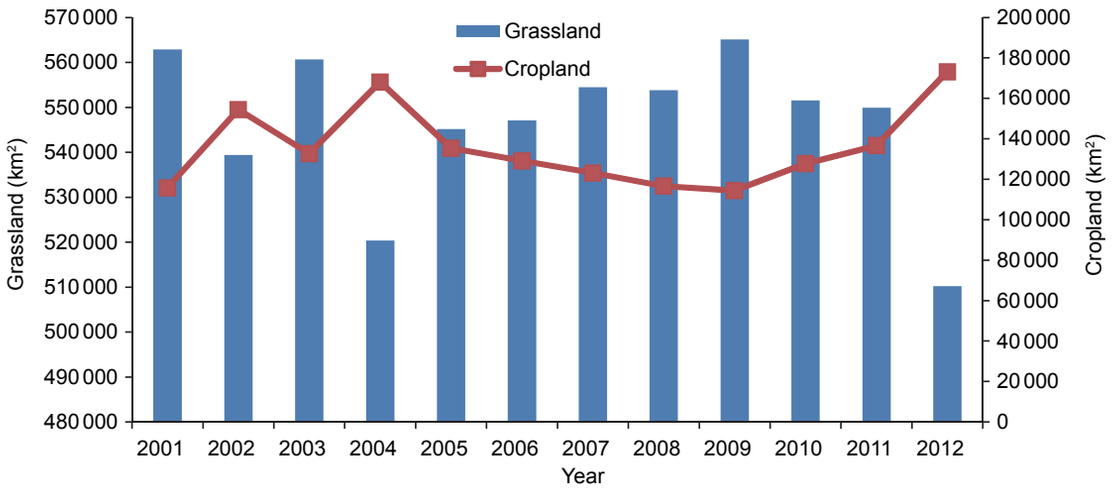

Fig. 3 Changes in the areas of grassland and cropland in the study area between 2001 and 2012.

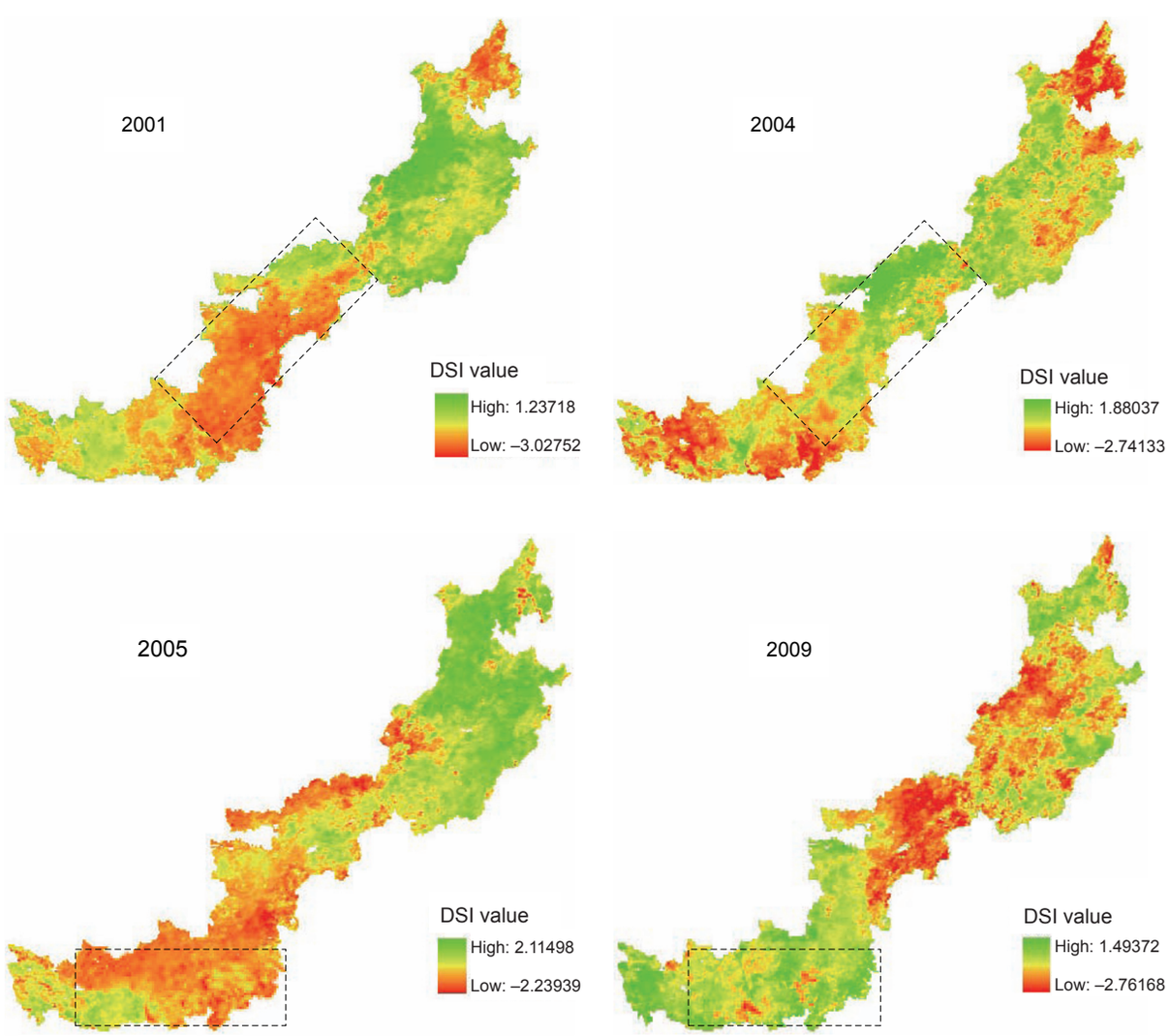

Fig. 4 Drought conditions in study area in 2001, 2004, 2005, and 2009. DSI, drought severity index.

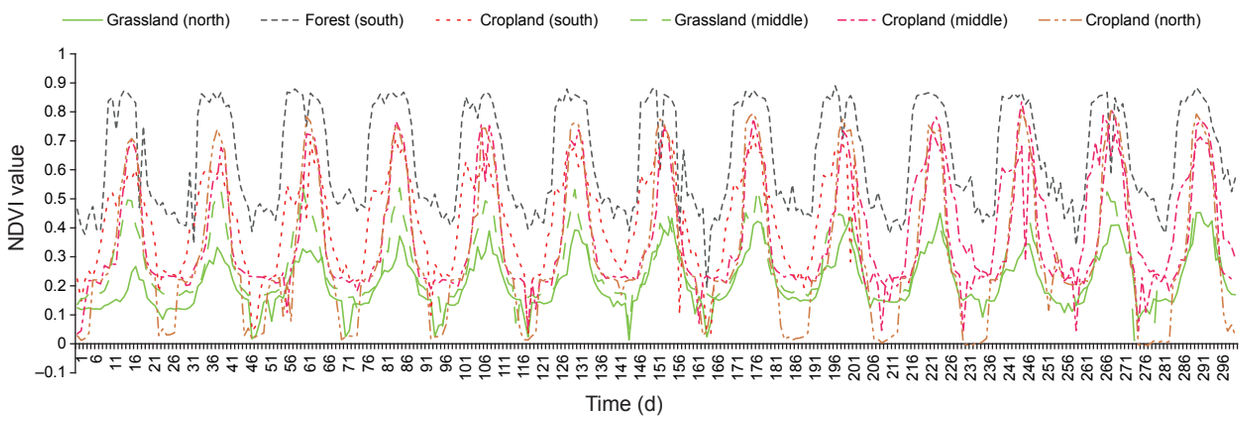

Fig. 5 Time series of the 16-d composite normalized-difference vegetation index (NDVI) values from 2001 to 2013 in six sample areas.

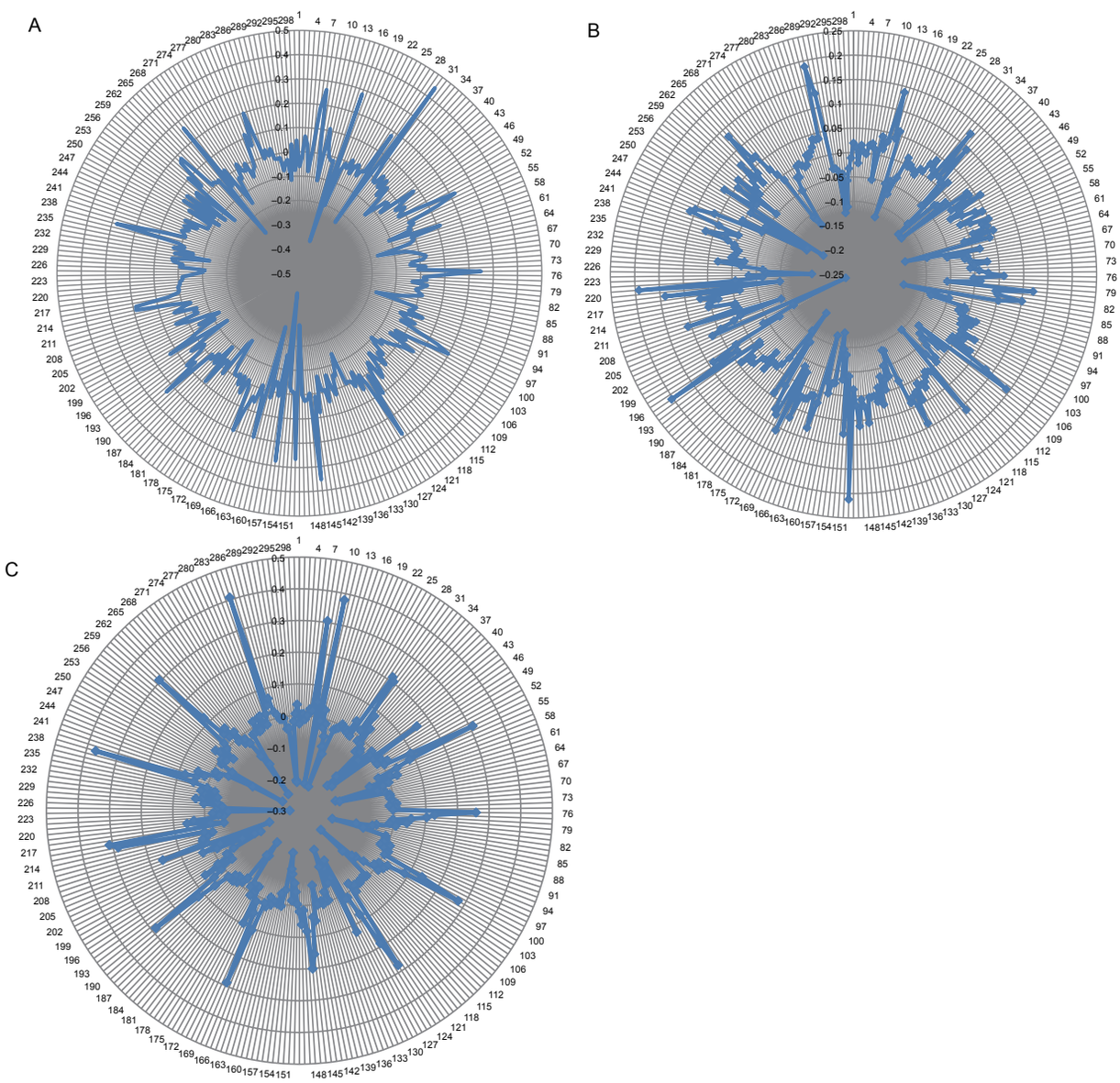

Fig. 6 Rate of change (ROC) of NDVI for different patterns of vegetation change: forest with no change (A), areas that changed from grassland to cropland (B) and changes in mixed/complex land cover type areas (C).

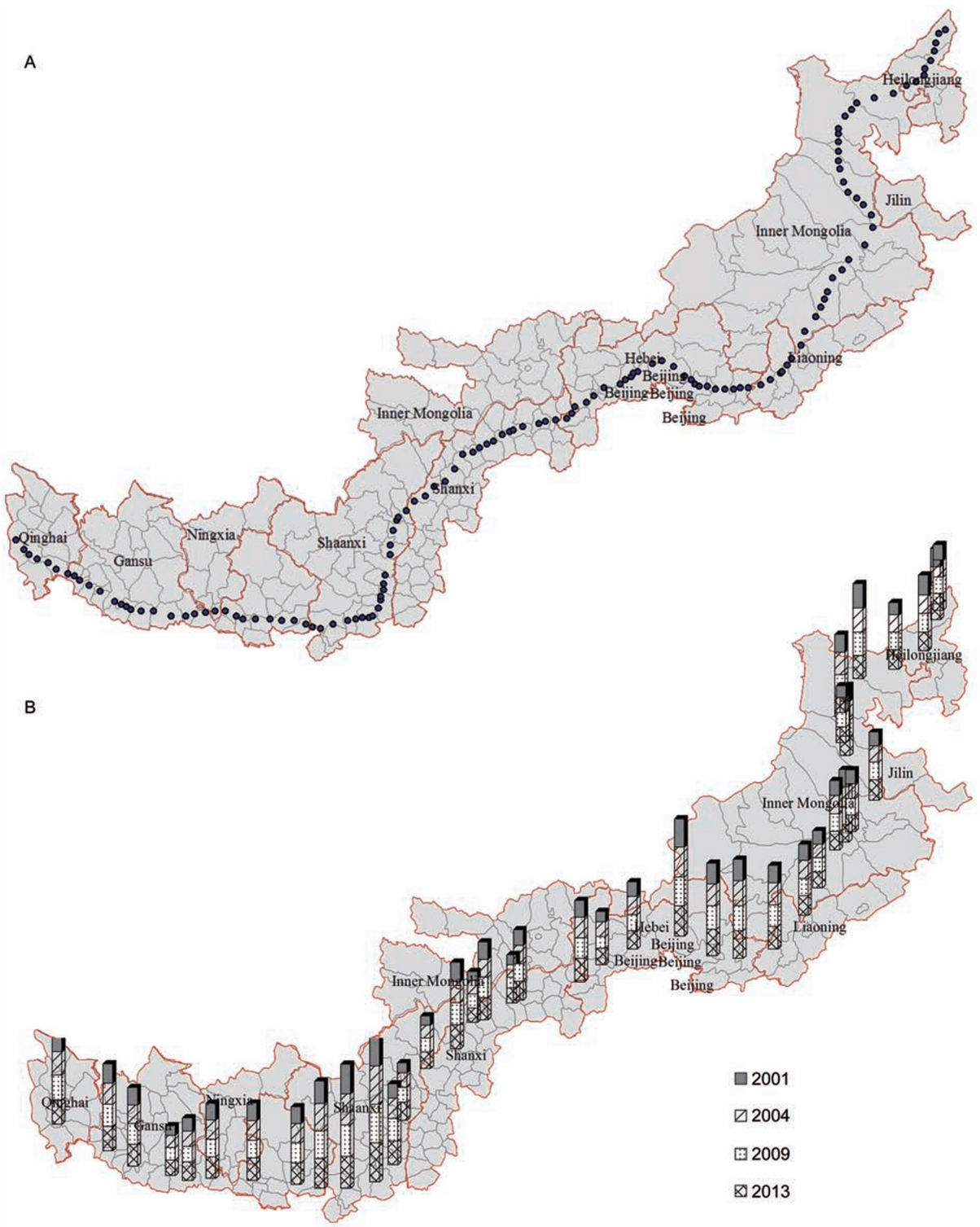

Fig. 7 Transect showing the sampling sites for the latitudinal and longitudinal variation in NDVI (A) and the corresponding changes in values in 2001, 2004, 2009, and 2013 (B).

in the northeast (Fig. 9), ranging between 100.874 and 124.773°E and between 34.72 to 48.455°N. The region is composed of 312 counties in 12 provinces, with a total area of 742 727 km^2. This ecotone lies near the northern 400 mm precipitation isoline. Precipitation in the northern and western regions of the ecotone ranges from 300 to

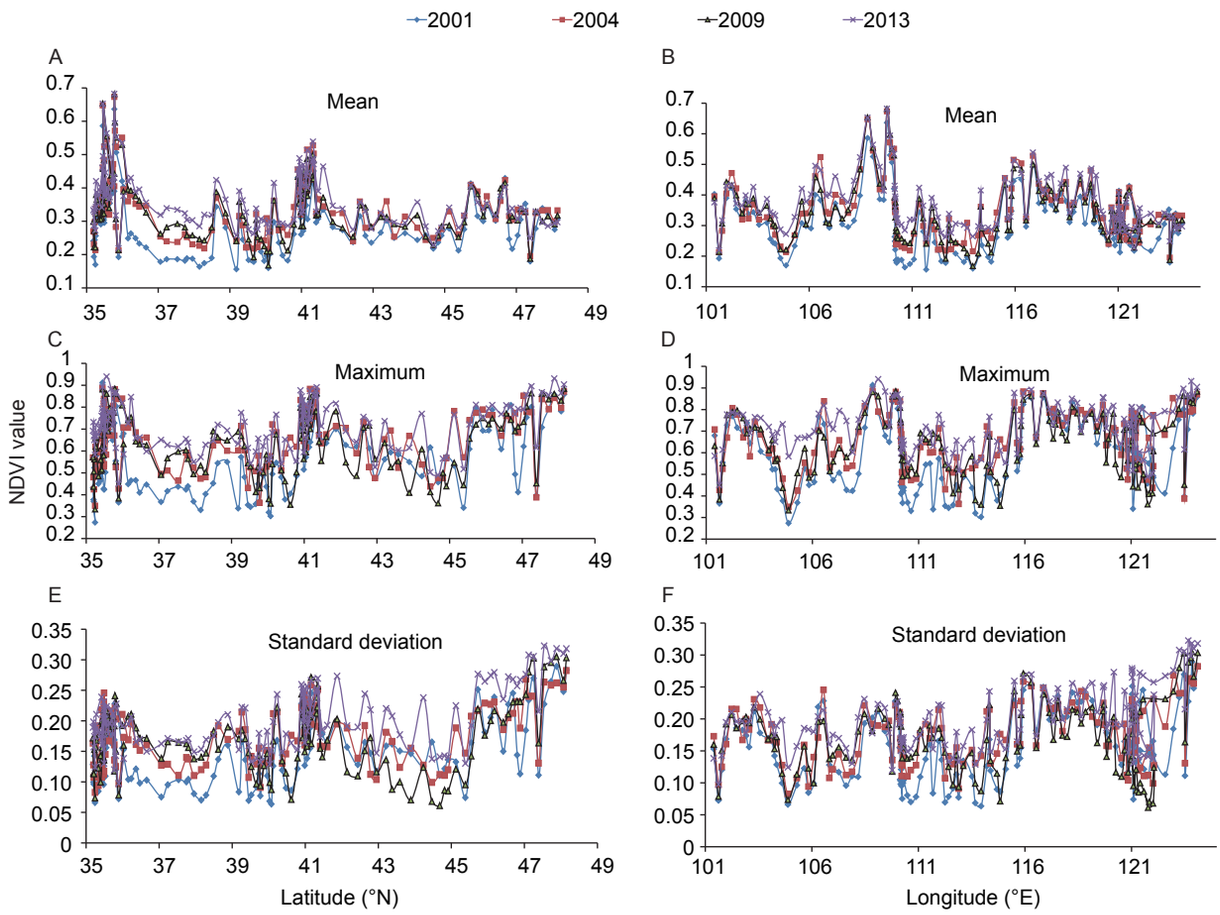

Fig. 8 Profiles of latitudinal and longitudinal variation in NDVI along the transect shown in Fig. 7.

400 mm, whereas precipitation in the southern and eastern regions ranges from 400 to 450 mm. However, annual precipitation varies greatly, ranging from 600 mm during wet years to 100 mm during drought years. There are also clear differences in annual mean temperatures between the southern and northern regions of the ecotone, ranging from 3.0 to 7.0°C in the eastern region, from 0.0 to 1.0°C in the central region, and from 6.0 to 9.0°C in the western region.

4.2. Remotely sensed data

MODIS land product data available by the United States Geological Survey Earth Resources Observation and Science are widely used in land use/cover change research (Poyatos *et al*. 2003; Shalaby and Tateishi 2007), landscape pattern analysis (Griffith *et al*. 2000), land surface biophysical parameter estimation (Masek *et al*. 2006), biochemical parameter estimation (Li *et al*. 2014), and vegetation monitoring (Li *et al*. 2014; Zhang *et al*. 2004). An extended and valuable time series of multi-temporal remote-sensing images is available for use (Klaric *et al*. 2012). Research results from Higginbottom and Symeonakis (2014) suggest that the most frequent use of Earth Observation data is for trend analysis of vegetation index data, most commonly by means of the NDVI as a proxy for net primary production (NPP) (Bi *et al*. 2013; Kim *et al*. 2014; Parida *et al*. 2014).

Accordingly, we used the 2001 to 2012 Collection 5 MODIS Land Cover Type product (MOD12Q1) (Friedl *et al*. 2002) to analyze changes in cropland and grassland areas, and used 2001 to 2013 MODIS NDVI data (MOD13A1) to analyze changes in vegetation cover, and use 2000 to 2011 MODIS DSI data (Mu *et al*. 2013) to descript the drought conditions in study area. The 16-d composite MOD13A1 product with 1-km resolution was used to illustrate seasonal changes in vegetation throughout the study period. The mean, maximum and standard deviation NDVI values were used to analyze annual changes in vegetation. All remotely sensed data were downloaded from the Land Processes Distributed Active Archive Center (URL: https://lpdaac.usgs.gov).

4.3. Meteorological data

We download the daily precipitation data and temperature

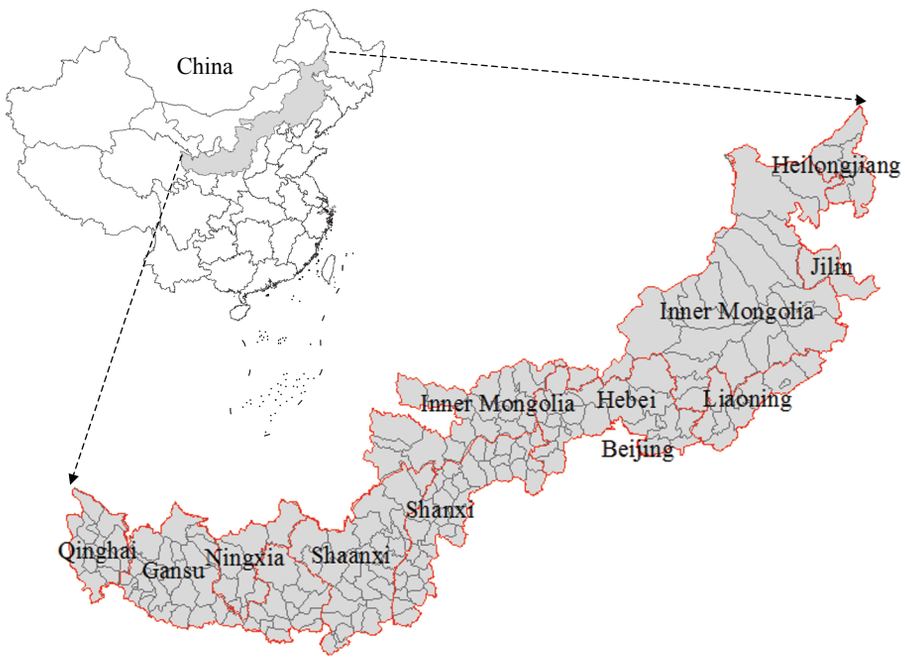

Fig. 9 Location of the study area and provincial boundaries.

data within the period from 2001 to 2013 coming from China Meteorological Science Data Sharing Service Network (URL: http://www.escience.gov.cn/metdata/page/index.html). And the Kriging interpolation method is used to the interpolation of these daily precipitation data and temperature point data with the 0.05° spatial resolution.

4.4. Methods

Long-term vegetation monitoring initiatives have become increasingly important tools for understanding ecosystem responses to climate change as well as to natural and anthropogenic disturbances (Sankey *et al*. 2015). Accordingly, we used NDVI time series to monitor vegetation growth in the study area. NDVI products with a 16-d temporal resolution and a 1-km spatial resolution were calculated using NDVI=$(\rho_{NIR}+\rho_R)/(\rho_{NIR}-\rho_R)$, where ρ represents the reflectance in the near-infrared (NIR) and red (R) bands. To minimize the effects of both cloud cover and view angle, we used the constrained view angle-maximum value composite (CV-MVC) method (Huete *et al*. 2011) in the MODIS vegetation index (VI) algorithm. Special care was taken for input data filtering. An NDVI threshold of 30% was used to constrain the absolute maximum value composite (MVC) deviations. Only the top two observations (i.e., those with maximum NDVI value) were used in the CV-MVC algorithm as a safeguard against outliers and cloud-contaminated observations. See the MODIS Vegetation Index Product Series Collection 5 Change Summary document (http://landweb.nascom.nasa.gov/QA_WWW/forPage/MOD13_VI_C5_Changes_Document_06_28_06.pdf) for more detailed information on the NDVI composite products.

To better monitor changes in vegetation cover, we used four types of annual NDVI composite products: the maximum, mean and standard deviation NDVI values during 23 phases of each year.

$$NDVI_{max}=Max(NDVI_1, NDVI_2, NDVI_3,\ldots, NDVI_{23})$$

$$NDVI_{mean}=\frac{\sum_{i=1}^{23} NDVI_i}{23}$$

$$NDVI_{SD}=\sqrt{\frac{1}{23}\sum_{i=1}^{23}\left(NDVI_i-Mean\left(NDVI_1, NDVI_2,..., NDVI_{23}\right)\right)^2}$$

Where, $NDVI_{max}$ is the maximum NDVI for each year (2001–2013); $NDVI_{mean}$ is the mean NDVI for each year for all phases; $NDVI_1$, $NDVI_2$, …, $NDVI_{23}$ are the 16-d MODIS NDVI composite images using the CV-MVC method; and $NDVI_{SD}$ is the standard deviation for the 23 phases.

In addition, we used the rate of change (ROC) to compare current NDVI values with NDVI values for the previous 16-d. ROC was calculated as follows:

$ROC=NDVI_{i+1}-NDVI_i$ (i=2, 3, …, 23)

We used the MOD12Q1 product to identify different land use and cover types (e.g., cropland, grassland, bodies of water, etc.), analyze changes in land use, and monitor changes in land cover. The MOD12Q1 product contains five classification schemes, which describe land cover properties

derived from observations spanning a year's input from the Terra and Aqua MODIS satellites. The primary land cover scheme identifies 17 classes defined by the International Geosphere-Biosphere Programme, which includes 11 natural vegetation classes, 3 developed and mosaicked land classes and 3 non-vegetated land classes. We applied this classification scheme. Because cropland and grassland were the dominant land cover types in this ecotone, we merged other land cover types. For example, evergreen needle-leaf forests, evergreen broadleaf forests, deciduous needle-leaf forests, deciduous broadleaf forests, and mixed forests were unified into a single forest type.

Acknowledgements

This research was funded by the National Basic Research Program of China (973 Program, 2014CB954301), the Project of the State Key Laboratory of Earth Surface Processes and Resources Ecology, Beijing Normal University, China (2013-KF-11) and the Project of Ministry of Environmental Protection of China (257228006).

References

Attrill M J, Rundle S D. 2002. Ecotone or ecocline: Ecological boundaries in estuaries. *Estuarine*, *Coastal and Shelf Science*, **55**, 929–936.

Battisti D S, Naylor R L. 2009. Historical warnings of future food insecurity with unprecedented seasonal heat. *Science*, **323**, 240–244.

Bi J, Xu L, Samanta A, Zhu Z, Myneni R. 2013. Divergent arctic-boreal vegetation changes between north america and eurasia over the past 30 years. *Remote Sensing*, **5**, 2093–2112.

Chen Y, Li X B, Su W, Li Y. 2008. Simulating the optimal land-use pattern in the farming-pastoral transitional zone of Northern China. *Computers*, *Environment and Urban Systems*, **32**, 407–414.

Dong J W, Tao F L, Zhang G L. 2011. Trends and variation in vegetation greenness related to geographic controls in middle and eastern Inner Mongolia, China. *Environment Earth Science*, **62**, 245–256.

Dong M Y, Jiang Y, Ren F P, Wu Z F. 2010. Variation trend and catastrophe change of air temperature in the farming-pastoral ecotone of northern China during recent 50 years. *Journal of Desert Research*, **30**, 926–932.

Dong T T, Zhang Z X, Qian F K. 2007. Dynamic change monitoring of cultivated land in a typical farming-pastoral ecotone in Northern China by remote sensing. *Transactions of the Chinese Society of Agricultural Engineering*, **23**, 78–82.

Ford J D, Pearce T. 2010. What we know, do not know, and need to know about climate change vulnerability in the western Canadian arctic: A systematic literature review. *Environmental Research Letters*, **5**, 75–82.

Friedl M A, Mciver D K, Hodges J C F, Zhang X Y, Muchoney D, Strahler A H, Woodcock C E, Gopal S, Schneider A, Cooper A, Baccini A, Gao F, Schaaf C. 2002. Global land cover mapping from MODIS: Algorithms and early results. *Remote Sensing of Environment*, **83**, 287–302.

Gong D Y, Han H. 2004. Extreme climate events in Northern China over the last 50 years. *Acta Geographica Sinica*, **59**, 230–238.

Griffith J A, Martinko E A, Price K P. 2000. Landscape structure analysis of Kansas at three scales. *Landscape and Urban Planning*, **52**, 45–61.

Higginbottom T P, Symeonakis E. 2014. Assessing land degradation and desertification using vegetation index data: Current frameworks and future directions. *Remote Sensing*, **6**, 9552–9575.

Huete A, Didan K, Leeuwen W, Miura T, Glenn E. 2011. MODIS vegetation indices. In: Ramachandran B, Justice C O, Abrams M J, eds., *Land Remote Sensing and Global Environmental Change*. vol. 11. Springer, New York. pp. 579–602.

John R, Chen J, Lu N, Wilske B. 2009. Land cover/land use change in semi-arid inner mongolia: 1992–2004. *Environmental Research Letters*, **4**, 549–567.

Karnieli A, Qin Z H, Wu B, Panov N, Yan F. 2014. Spatio-temporal dynamics of land-use and land-cover in the Mu Us sandy land, China, using the change vector analysis technique. *Remote Sensing*, **6**, 9316–9339.

Kent M, Gill W J, Weaver R E, Armitage R P. 1997. Landscape and plant community boundaries in biogeography. *Progress in Physical Geography*, **21**, 315–353.

Kim Y, Kimball J S, Didan K, Henebry G M. 2014. Responses of vegetation growth and productivity to spring climate indicators in the conterminous United States derived from satellite remote sensing data fusion. *Agricultural and Forest Meteorology*, **194**, 132–143.

Klaric M N, Anderson B, Shyu C R. 2012. Information mining from human visual reasoning about multi-temporal, high-resolution satellite imagery. *International Journal of Image and Data Fusion*, **3**, 243–256.

Li L, Friedl M A, Xin Q C, Gray J, Pan Y Z, Frolking S. 2014. Mapping crop cycles in China using MODIS-EVI time series. *Remote Sensing*, **6**, 2473–2493.

Liu J H, Gao J X, Lv S H, Han Y W, Nie Y H. 2011. Shifting farming — pastoral ecotone in China under climate and land use changes. *Journal of Arid Environments*, **75**, 298–308.

Masek J G, Vermote E F, Saleous N E, Wolfe R, Hall F G, Huemmrich K F, Gao F, Kutler J, Lim T K. 2006. A Landsat surface reflectance dataset for North America, 1990–2000. *IEEE Geoscience and Remote Sensing Letters*, **3**, 68–72.

Mu Q Z, Zhao M S, Kimball J S, McDowell N G, Running S W. 2013. A remotely sensed global terrestrial drought severity index. *Bulletin of the American Meteorological Society*, **94**, 83–98.

Parida B R, Buermann W. 2014. Increasing summer drying in North American ecosystems in response to longer

nonfrozen periods. *Geophysical Research Letters*, **41**, 5476–5483.

Poyatos R, Latron J, Llorens P. 2003. Land use and land cover change after agricultural abandonment: The case of a Mediterranean mountain area (Catalan Pre-Pyrenees). *Mountain Research and Development*, **23**, 362–368.

Richardson A D, Keenan T F, Migliavacca M, Ryu Y, Sonnentag O, Toomey M. 2013. Climate change, phenology, and phenological control of vegetation feedbacks to the climate system. *Agricultural and Forest Meteorology*, **169**, 156–173.

Rudel T K, Coomes O T, Moran E, Achard F, Angelsen A, Xu J, CLambin E. 2005. Forest transitions: Towards a global understanding of land use change. *Global Environmental Change*, **15**, 23–31.

Sankey J B, Munson S M, Webb R H, Wallace C S A, Duran C M. 2015. Remote sensing of Sonoran Desert vegetation structure and phenology with ground-based LiDAR. *Remote Sensing*, **7**, 342–359.

Sellers P, Hall F, Margolis H, Kelly B, Baldocchi D, den Hartog G, Cihlar J, Ryan M G, Goodison B, Crill P, Ranson K J, Lettenmaier D, Wickland D E. 1995. The boreal ecosystem-atmosphere study (BOREAS): An overview and early results from the 1994 field year. *Bulletin of the American Meteorological Society*, **76**, 1549–1577.

Shalaby A, Tateishi R. 2007. Remote sensing and GIS for mapping and monitoring land cover and land-use changes in the Northwestern coastal zone of Egypt. *Applied Geography*, **27**, 28–41.

Tao F L, Zhang Z. 2010. Dynamic responses of terrestrial ecosystems structure and function to climate change in China. *Journal of Geophysical Research* (Biogeosciences), **115**(G3), 58–72.

Tao F L, Zhang Z, Xiao D P, Zhang S, Rötter R P, Shi W J, Liu Y J, Wang M, Liu F S, Zhang H, Zhao H L, Zhao X Y, Zhang T H, Zhou R L. 2014. Responses of wheat growth and yield to climate change in different climate zones of China, 1981–2009. *Agricultural and Forest Meteorology*, **189**, 91–104.

Zhang W B, Liu B Y. 2003. Spatial distribution of precipitation extremum in the ecotone between agriculture and animal husbandry in northern China. *Journal of Natural Resources*, **18**, 274–280.

Zhang X Y, Friedl M A, Schaaf C B, Strahler A H, Schneider A. 2004. The footprint of urban climates on vegetation phenology. *Geophysical Research Letters*, **31**, L12209.

Zhao H L, Zhao X Y, Zhang T H, Zhou R L. 2002. Boundary line on agro-pasture zig zag zone in north China and its problems on eco-environment. *Advances in Earth Science*, **17**, 739–747.

(Managing editor WANG Ning)